

2

FTD-ID(RS)T-0718-89

AD-A216 796

# FOREIGN TECHNOLOGY DIVISION

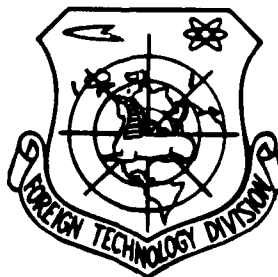


DTIC  
ELECTE  
JAN 12 1990  
S DCS D

INSPECTION OF CARBON/EPOXY AND ALUMINUM HONEYCOMB PARABOLOIDAL COMPONENTS  
BY HNDT

by

Huang Guanhua, Wei Ensheng

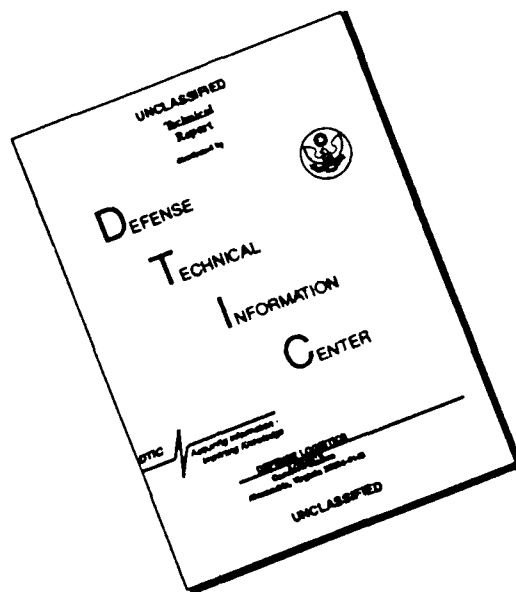


Approved for public release;  
Distribution unlimited.



90 01 11 053

# DISCLAIMER NOTICE



THIS DOCUMENT IS BEST QUALITY AVAILABLE. THE COPY FURNISHED TO DTIC CONTAINED A SIGNIFICANT NUMBER OF PAGES WHICH DO NOT REPRODUCE LEGIBLY.

## HUMAN TRANSLATION

FTD-ID(RS)T-0718-89 21 September 1989

MICROFICHE NR: FTD-89-C-000781

INSPECTION OF CARBON/EPOXY AND ALUMINUM  
HONEYCOMB PARABOLOIDAL COMPONENTS BY HNDD

By: Huang Guanhua, Wei Ensheng

English pages: 6

Source: Nondestructive Testing, Vol. 10, Nr. 3  
March 1988, pp. 69-71

Country of origin: China

Translated by: Leo Kanner Associates  
F33657-88-D-2188

Requester: FTD/TQTAV/Jeffery D. Locker

Approved for public release; Distribution unlimited.

THIS TRANSLATION IS A RENDITION OF THE ORIGINAL FOREIGN TEXT WITHOUT ANY ANALYTICAL OR EDITORIAL COMMENT. STATEMENTS OR THEORIES ADVOCATED OR IMPLIED ARE THOSE OF THE SOURCE AND DO NOT NECESSARILY REFLECT THE POSITION OR OPINION OF THE FOREIGN TECHNOLOGY DIVISION.

PREPARED BY:

TRANSLATION DIVISION  
FOREIGN TECHNOLOGY DIVISION  
WPAFB OHIO

# GRAPHICS DISCLAIMER

All figures, graphics, tables, equations, etc. merged into this translation were extracted from the best quality copy available.



Accession For	
NTIS CRA&I	<input checked="" type="checkbox"/>
DTIC TAB	<input type="checkbox"/>
Unannounced	<input type="checkbox"/>
Justification	
By	
Distribution/	
Availability Codes	
Dist	Avail and/or Special
A-1	23

Huang Guanhua, Wei Ensheng  
Space Ministry Laboratory 703

→ This paper discusses examples of the use of the double-exposure method to inspect carbon/epoxy skin and aluminum honeycomb core paraboloidal components.

CONT'D Pg. 16

## 1. TESTING EQUIPMENT AND METHODS

### 1.1 Lithographic Plate Samples with Artificial Defects

The material and construction of the lithographic plate samples with artificial defects were the same as for the bona fide product. The skin thickness was 0.5 mm, and eight defects, arranged in two rows, were present on each sample. In size, the four defects in each row corresponded to those of the other row, being respectively 30, 20, 15, and 10mm (see Fig. 1). The samples included two types of defects, the separated style and the closely attached style.

For the separated style defects, the glue layer is removed in the defect location; a thin polytetrafluorethane film replaces it (Fig. 2).

The closely attached style defects do not involve a removal of the glue layer in the defect location, but instead a thin film of polytetrafluorethane is squeezed between the glue layer and the skin (Fig. 3).

---

#### Translator's note:

Note in original: Our colleagues Zhang Jie and Qian Ziqiang participated in these experimentations.

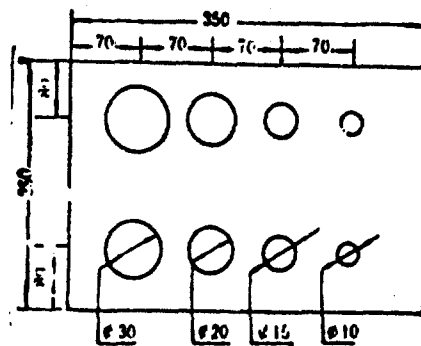


Fig. 1. Lithographic plate sample with artificial defects.

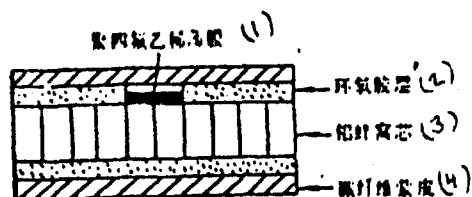


Fig. 2. Separation style defect structure. Key: (1) Polytetrafluoroethylene film; (2) Epoxy glue layer; (3) Aluminum honeycomb core; (4) Carbon fiber skin.

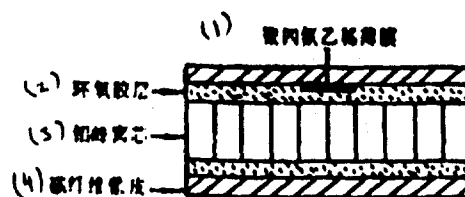


Fig. 3. Closely attached style defect structure. Key: (1) Polytetrafluoroethylene film; (2) Epoxy glue layer; (3) Aluminum honeycomb core; (4) Carbon fiber skin.

## 1.2. Paraboloidal Components

Paraboloidal components are local elliptical circles, with a skin thickness of 0.35 mm; the long axis of the elliptical circles is 1.2 m and the short axis 0.7 m. There are a convex and concave face.

## 1.3 Light Path

1) The object beam reflector of the concave surface light path and the holographic dry plate are respectively placed near the two focal points of the paraboloidal surface. This allows the dry plate to receive the most intense object beam, at the same time insuring that the object beam at all points is generally equal. Because the distance between the focal point and the object is rather large at this time, the concave face only requires one photograph for complete measurement.

2) The convex face light path holographic plate is placed near the location of the object. In this way, we overcome the defect of the convex face divergent light being rather weak when it reached the dry plate location. But the photographic surface area is correspondingly reduced, and the number of photographs required is correspondingly increased.

The holographic dry plate is not placed where the light reflected by the object is the most intense, but rather where the reflected light is relatively even. Because at the point where light reflected by the convex surface is strongest the light field is not even, because the mid-range light near the optical surface is reflected, and because the light in the border regions is very weak, the photograph's quality is very poor.

#### 1.4. Loading

The loading methods for holographic EMT normally include mechanical, pressure, shock and thermal stress methods. Of these, the thermal stress method has the advantage of being simple, convenient, and rapid. This paper therefore uses the thermal stress method.

#### 1.5. Photography

For our experiments we selected the composite real-time/double-exposure method. The real-time method is used to discover the loading conditions; the double-exposure method is used to record the final experimental results. The double-exposure method involves first making one exposure of the object, and then, after using an electrical hair dryer to heat the surface of the object until an appropriate deformation is obtained, making a second exposure, and finally processing the dry plate, producing a double-exposure holographic image.

## 2. RESULTS AND ANALYSIS

### 2.1 Test Conditions

For our experiments we used a 50 mW neon laser apparatus for our light source. The ratio of the intensity of the object beam and the reference beam was between 1:2 and 1:4. The interval between the two exposures was three minutes, and the angle between the two light beams was  $30^\circ$  to  $45^\circ$ .

### 2.2 Test Results

Figures 4 through 8 are all double-exposed holographic images. Each experiment used the electrical hair dryer to provide heat. In Fig. 6, the heating duration was 45 seconds; for the others it was one minute. The defect location in the images is indicated by an arrow.

### 2.3. Analysis

It can be seen from Fig. 4 and Fig. 5 that all eight separation style defects appear, while six of the closely attached defects appear, the two 10cm being the exception. This is because the hollow area in the separation style defects is large, and a great amount of air exists inside them; while for the closely attached style defects there is very little air inside. After heating, the air in the defect areas expands, so the separation style defects show greater deformity than the closely attached style defects.

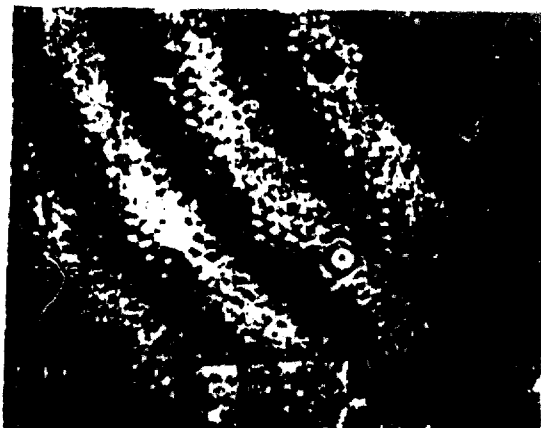


Fig. 4. Separation style defect sample.

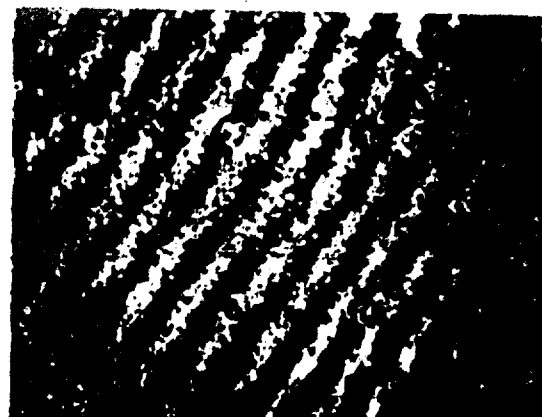


Fig. 5. Closely attached style defect sample.

Figures 6 and 7 are holographic images of the two faces of the same paraboloidal surface. Each of them has an abnormal region whose size is completely equivalent. Examination reveals that the abnormal regions of the



Fig. 6. Holograph of paraboloidal convex surface.



Fig. 7. Holograph of paraboloidal convex surface.

two photographs are in the same position. Figure 8 represents an X-ray investigation of the abnormal area; the product list shows that this location in the honeycomb system is filled with foamed plastic.

Examination was undertaken on the defects in an area of about 7 by 5 cm. Four photographs were made, and the repetivity was good. The explanation for this is that on large area surfaces the glue-loss defects are easily detected by the holographic method. These defects are not detected using the X-ray method or the sound-blocking method.

In the experiment, it also appeared that the heating amount of the convex face was slightly greater than that of the concave face. This may be because the thermal expansion coefficient of carbon fiber is a negative value, so the skin in the defect regions of the concave surface, when being heated, may change from curved to straight, separate from the core, and produce a rather great deformity of the defect area surface.

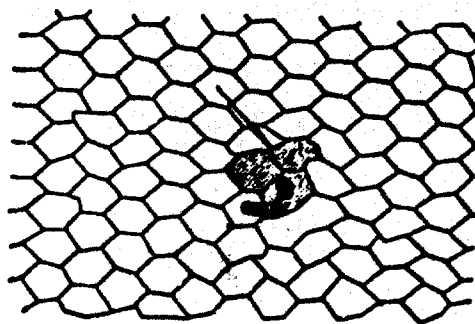


Fig. 8. X ray of number 3 paraboloid surface.

## CONCLUSIONS

*cont'd*

1. Laser holographic technology can detect separation style and closely attached style glue-loss defects, but its sensitivity in detecting the closely attached style defects is lower than its sensitivity in detecting the separation style defects.

2. Laser holographic technology has the capacity of detecting confused areas within the honeycomb core, but the results are not so good as with direct X-ray observation.

*Keywords: Lithographic Plates, Defects materials, Translations, China, Chinese Language.*

## REFERENCE MATERIAL

1. Chen Jirao, Yu Wanting. Nondestructive testing of glued structure and compound materials, National Defense Industry Publishing House, 1984.
2. Erf, Robert K. Holographic nondestructive testing, p. 225, New York Academic Press, 1974.
3. Wu Linlin, Wang Renda et al. "A study of holographic testing methods for carbon fiber speaker antennas," Jiguang Quanxi Liankan [United Laser Holographic Journal], No. 4, Vol. 4., 1984.
4. Engineering Mechanics Department of Qinghua University. Laser holographs and speckle interference measurement, 9, 1983.

# DISTRIBUTION LIST

## DISTRIBUTION DIRECT TO RECIPIENT

<u>ORGANIZATION</u>	<u>MICROFICHE</u>
A205 DMAHTC	1
C509 BALLISTIC RES LAB	1
C510 R&T LABS/AVEADCOM	1
C513 ARRADCOM	1
C535 AVRADCOM/TSARCOM	1
C539 TRASANA	1
C591 FSTC	4
C619 MIA REDSTONE	1
D008 MISC	1
E053 HQ USAF/INET	1
E404 AEDC/DOF	1
E408 AFWL	1
E410 AD/INP	1
F429 SD/INT	1
P005 DOE/ISA/DOJ	1
P050 CIA/OCR/ADP SD	2
AFIT-LFF	1
FTD	
CCV	1
MIA/PHS	1
LLYL/CODE 1-560	1
NASA/NST-44	1
NSA/TS13/TDL	2
ASD/FTD TOLA	1
FSL/NIX-3	1
NOIC/OIC-9	1